characteristics of PAHs and NPAHs distribution in Hanoi as a typical motorbike city in the world by comparing with those in automobile and coal-burning cities.

EXPERIMENTAL METHODS

Hanoi City and Sampling Sites Description

Hanoi is an economic and industrial center of Vietnam, with more than 6 million inhabitants in the area of about 3,324 square km. Being influenced by the Southeast Asia monsoon regime, the climate is tropical and humid. Summer, from May to September, is hot (average temperature 32°C) with plenty of precipitation, while winter, from November to March, is not so cold (average temperature 14°C) and relatively dry. The average annually humidity is 79% and rainfall is 1,800 mm a year (24). Motorbikes are the chief means of transportation in Vietnam. In Hanoi, where there is about 1 motorbike for every 2 people, motorbikes account for more than 90% of total vehicles (25–27) and cause traffic jams and air pollution.

Airborne particulates were collected at two representative sites in Hanoi city using a 120H high-volume air sampler (Kimoto Electric Company Limited, Osaka, Japan) at a flow rate of 1,000 L min^{-1}. The first sampling site (site I, the latitude and longitude is N: 20°59.854′; E: 105° 48.804′) was on the rooftop of a building 10 m above ground level. This site is located in a mixed residential, commercial, and institutional area next to the only old inner-city industrial zone remaining in the center of Hanoi city. The second sampling site (site T, the latitude and longitude is N: 210°03.570′; E: 105° 47.006′) was in the balcony of a second-story building (approximately 4 m above ground level). This building was 3 m from one of heaviest traffic streets in Hanoi, and 15 m from the intersection of Pham Van Dong-Co Nhue. This intersection is one of the busiest of Hanoi city with heavy traffic jams (25,28).

Sampling

The total particulate matter (TPM) samples were collected on Pallflex 2500QAT-UP membrane filters, 8 × 10 in. The sampling was started from 10 am and conducted over a continuous period of 24 h in 7 consecutive days in summer (August 19–25, 2010) and winter (February 13–19, 2011). The filters were kept in desiccators at room temperature within 48 h and weighed before and after sampling. Each filter was wrapped in aluminum foil and put in a sealable plastic bag and kept in a refrigerator at −20°C until use.

Chemicals

The EPA 610 Polynuclear Aromatic Hydrocarbons standard mixture including naphthalene (Nap), acenaphthalene (Ace), fluorene (Fle), phenanthrene (Phe), anthracene (Ant), fluoranthene (Flu), pyrene (Pyr), benz[*a*]anthracene (B*a*A), chrysene (Chr), benzo[*b*]fluoranthene (B*b*F), benzo[*k*]fluoranthene (B*k*F), benzo[*a*]pyrene (B*a*P), dibenz[*a,h*]anthracene (DBA), benzo[*ghi*]perylene (B*ghi*Pe) and indeno[*1,2,3-cd*]pyrene (IDP) were purchase from Supelco Park – U.S.A. The standard mixture of 17 NPAHs including 1,3-, 1,6-, 1,8-dinitropyrene (DNPs), 3-nitrobenzanthrone (3-NBA), 2-nitrofluorene (2-NF), 9-nitrophenanthrene (9-NPh), 2-nitroanthracene (2-NA), 9-nitroanthracene (9NA), 1-nitropyrene (1-NP), 3-nitrofluoranthene (3-NFR), 1-nitrofluoranthene (1-NFR), 2-nitrotriphenylene (2-NTP), 6-nitrochrysene (6-NC), 7-nitrobenz[*a*]anthracene (7-NB*a*A), 6-nitrobenzo[*a*]pyrene (6-NB*a*P), 1-nitroperylene (1-NPer) and 3-nitroperylene (3-NPer) were purchased from AccuStandard, Inc., New Haven, U.S.A. Five deuterated PAHs (Nap-d_8, Ace-d_{10}, Phe-d_{10}, Pyr-d_{10} and Bap-d_{12}) were purchased from Wako Pure Chemical Industries, Ltd., (Osaka, Japan) as internal standards for PAHs analysis. All of these compounds were dissolved in acetonitril with different concentrations. 2-Fluoro-7-nitrofluorene (FNF) was purchased from Aldrich Chemical Company, Inc. (Milwaukee, WI) as an internal standard for NPAHs analysis. All solvents and other chemicals were HPLC or analytical grade purchased from Wako Pure Chemical Industries, Ltd and Kanto Chemical Company (Tokyo, Japan).

PAHs and NPAHs Analysis by High-Performance Liquid Chromatography (HPLC)

A piece of 1 × 5 in (for PAHs) and 2 × 5 in (for NPAHs) of each filter (8 × 10 in) was thoroughly cut into small pieces (0.02 in square) and put in a flask. Internal standards for PAHs and NPAHs were added to the flask with the volume of 100 μl. Both PAHs and NPAHs on filter papers were extracted ultrasonically twice with 40 ml benzene/ethanol (3:1, v/v) and the extracted solution was filtered by a filter paper (Advantec, Toyo No. 6, 125 mm diameter, Toyo Roshi Kaisha, Ltd., Tokyo, Japan) and a membrane filter (HLC-Disk 13, pore size 0.45 μm). The filtrate was washed with 80 ml of 5% sodium hydroxide solution, 80 ml of 20% sulfuric acid solution, and 80 ml distilled water, successively. After the washing step, the filtrate was evaporated to dryness in a round bottom flask with 100 μl dimethyl sunfoxide. In the case of PAHs, the residue was dissolved in 900 μl acetonitril, and for NPAHs, the residue was dissolved in 900 μl ethanol. Finally, the extract was passed through a membrane filter (HLC-Disk 13, pore size 0.45 μm) and then 100 μl solution was injected into the HPLC system.

Fifteen PAHs were determined by using an HPLC with a fluorescence detector. The system consists of two HPLC pumps (LC-10AD, Shimadzu, Kyoto, Japan), a fluorescence detector (RF-10A, Shimadzu), a system controller (SCL-10A, Shimadzu), an integrator (Chromatopac C-R7Ae, Shimadzu), an auto sample injector (SIL-10A, Shimadzu), a column oven (CTO-10AS, Shimadzu), a guard column (Inertsil ODS-P, 4.0 i.d. × 10 mm, GL Sciences Inc., Tokyo, Japan), and an analytical column (Inertsil ODS-P, 4.6 i.d. × 250 mm, GL Sciences Inc.). The mobile phase was acetonitrile/water with an increasing acetonitrile concentration. The time program of the fluorescence detector was set to detect at the optimum excitation and emission wavelengths for each PAH according to our previous report (29).

Eleven primary formed NPAHs were determined by using an HPLC with a chemiluminescence detector (CLD-10A, Shimadzu, Japan) and a switching-column according to the procedure described in our previous studies with some modifications (30). The system consists of 6 HPLC columns: a guard column 1 (4.6 × 30 mm, 20°C), a guard column 2 (4.6 × 50 mm, 20°C), a clean-up column (4.6 × 150 mm, 20°C), a reducer column (Pt/Rh, 4.0 × 10 mm, 80°C), a concentrator column (4.6 × 30 mm, 20°C), and a separator column (4.6 × 250 mm, 20°C). The mobile phase for the concentrator column was imidazole-$HClO_4$ buffer (pH 7.6)/acetonitrile and the mobile phase for reducer and clean up columns was an ethanol/acetate buffer (3:1, v/v). The validity of the NPAH determination method was confirmed in our previous reports (30). The recoveries of NPAHs varied from 82–106%, the limits of detection (S/N = 3) varied from 0.25–1.5 fmol, and the limits of quantification (S/N = 10) varied from 10^{-15}–10^{-12} mol (over two orders) with good linearities ($r^2 > 0.899$) (29,30).

RESULTS AND DISCUSSION

PAHs and NPAHs Occurrence

Fifteen PAHs were determined for all samples. PAHs with 2 and 3 rings were partially lost from the filters because of their higher volatility, and so their measured concentrations were less than the true concentrations. Furthermore, the PAHs with low molecular weight are often less carcinogenic than those with high molecular weight. From these reasons, we focused on 10 PAHs having 4, 5, and 6 rings associated with airborne particulates only. The mean concentrations and standard deviations of PAHs at two sites are shown in Table 1. The total concentration of 10 PAHs at site T was about four times the concentration at site I in summer but only about half the concentration at site I in winter. The most abundant PAH at both sites in both seasons was the 6-ring B*ghi*Pe. At site I, the annual average concentration of predominant PAHs was in the order: B*ghi*Pe > IDP > B*b*F in summer and B*ghi*Pe > B*b*F >

Table 1: PAH concentrations (pmol m^{-3}) in Hanoi City

		Site I		Site T	
PAH[a]	Ring number	Summer	Winter	Summer	Winter
Flu	4	0.25 ± 0.28	5.52 ± 1.60	2.09 ± 0.24	2.03 ± 1.04
Pyr		0.44 ± 0.24	6.68 ± 1.87	3.36 ± 0.39	2.32 ± 1.24
B*a*A		0.33 ± 0.19	3.26 ± 0.85	2.33 ± 0.49	1.59 ± 1.09
Chr		0.46 ± 0.21	5.43 ± 1.32	3.52 ± 0.78	3.18 ± 1.56
B*b*F	5	1.22 ± 0.59	9.54 ± 2.47	5.62 ± 1.99	4.14 ± 1.95
B*k*F		0.45 ± 0.24	3.81 ± 1.02	2.05 ± 0.66	1.43 ± 0.87
B*a*P		0.79 ± 0.45	5.29 ± 1.67	5.59 ± 3.40	1.26 ± 0.84
DBA		0.48 ± 0.63	1.60 ± 0.37	0.97 ± 0.36	0.99 ± 0.48
B*ghi*Pe	6	2.65 ± 1.36	13.3 ± 4.80	11.4 ± 3.39	4.75 ± 2.98
IDP		2.57 ± 1.98	9.24 ± 2.55	4.99 ± 2.12	3.07 ± 2.34
Total PAHs		9.6 ± 6.2	63.7 ± 18.5	41.9 ± 13.8	± 14.4

[a] All data show mean ± SD.

IDP in winter. At site T, the order was: B*ghi*Pe > B*b*F > B*a*P in summer and B*ghi*Pe > B*b*F > IDP in winter.

Nine NPAHs were found at site I and 11 NPAHs were found at site T (Table 2). The total concentration of 11 NPAHs at site T was about eight times the total concentration of 9 NPAHs at site I in summer but only about half the concentration at site I in winter. Atmospheric NPAHs can be roughly divided into two groups: primary NPAHs found in diesel engines exhaust such as 1,3-, 1,6-, 1,8-DNPs, 1-NP, 6-NC, 9-NA (10), and secondary NPAHs formed in the atmosphere: 2-NFR and 2-NP. In this study, we focused only primary NPAHs.

Table 2: NPAH concentrations (fmol m^{-3}) in Hanoi City

		Site I		Site T	
NPAH[a]	Ring number	Summer	Winter	Summer	Winter
2-NA	3	NQ[b]	NQ[b]	9.31 ± 1.83	NQ[b]
9-NA		42.2 ± 31.9	552 ± 217	83.5 ± 34.3	236 ± 129
1,6-DNP	4	0.11 ± 0.08	0.16 ± 0.07	0.68 ± 0.21	0.09 ± 0.04
1,8-DNP		0.61 ± 0.32	1.21 ± 0.23	3.25 ± 0.88	0.71 ± 0.46
1,3-DNP		1.50 ± 1.06	1.73 ± 0.69	3.10 ± 1.19	0.74 ± 0.44
1-NP		29.1 ± 18.1	170 ± 64.7	488 ± 86.0	175 ± 121
6-NC		NQ[b]	NQ[b]	125.8 ± 30.8	NQ[b]
7-NBaA		41.2 ± 36.2	214 ± 105	167 ± 45.8	94.2 ± 43.1
1-NPer	5	0.42 ± 0.34	1.41 ± 0.62	1.87 ± 1.29	0.73 ± 0.45
3-NPer		1.71 ± 0.94	6.61 ± 0.87	11.2 ± 2.32	3.70 ± 1.59
6-NBaP		4.29 ± 3.13	18.1 ± 5.18	30.9 ± 6.34	13.0 ± 7.18
Total NPAHs		121 ± 92.0	965 ± 394	925 ± 211	524 ± 303

[a] All data show mean ± SD.
[b] NQ: detected but not quantified.

9-NA, 1-NP, and 7-NBaA were the most abundant NPAHs at both sites. Among them, small peaks of 2-NA and 6-NC were detected but not quantified in several samples because of the presence of interfering peaks. The highest NPAH at both sites was 9-NA except for 1-NP in winter at site T. Many studies have found that the most abundant NPAH in diesel and gasoline exhausts is 1-NP and it is not easily formed through gas-phase reactions (10,31). The level of 1-NP at site T, averaged over the year, was 331 ± 103 fmol m^{-3}, about 3 times the average level at site I (99.6 ± 41.4 fmol m^{-3}). Taking into consideration the fact that 1-NP is emitted mainly from diesel and gasoline engines, Table 2 suggested that the contribution of motor vehicles were much stronger at site T than site I.

PAH and NPAH levels in airborne particulates in summer were considerably different from those in winter. In general, the seasonal variation of PAHs and NPAHs depends on the changes of emission sources, weather conditions and secondary chemical reactions. Many studies have found that the levels of PAHs and NPAHs in winter were higher than those in summer due to the stability of the atmospheric layers in winter, the stronger photochemical reactions in summer and the increase in coal or kerosene combustion amount in winter (3,8,9). In our study, at site I, the concentrations of individual PAHs and NPAHs in winter were higher than those in summer. On the contrary, at site T, both PAH and NPAH levels in summer were higher than those in winter, probably as a result of seasonal changes in wind direction. However, the composition ratios of NPAH and PAH at both sites were not very different.

Emission Sources

Molecular diagnostic ratios are often used to identify emission sources of PAHs and NPAHs in the atmosphere. We have reported that [NPAH]/[PAH] concentration ratios of three pairs, [6-NBaP]/[BaP], [7-NBaA]/[BaA], and [1-NP]/[Pyr] are useful for identifying the contributors because the formation of NPAHs depends on the combustion temperature, increasing significantly with rising combustion temperature (29). Among these ratios, [6-NBaP]/[BaP] is a valuable diagnostic marker since BaP is frequently monitored as a carcinogen. In addition, BaP, which is non-volatile, exists only in the particulate phase in the atmosphere. In this report, [6-NBaP]/[BaP] concentration ratio was 0.44×10^{-2} and 0.80×10^{-2} at sites I and T, respectively (Table 3). These values were similar to the values of Kanazawa, a typical automobile city in Japan, (0.83×10^{-2} in summer and 0.8×10^{-2} in winter) during 1999 and 2010 (32). The combustion temperature of motorbike engines is almost the same as that of motor vehicle engines (around 2700–3000°C). This suggests that the ratio of [NPAH]/[PAH] might be similar in particulates both from motorbikes and motor vehicles and the contribution of motorbikes was relatively stronger at site T than site I.

Table 3: Diagnostic ratios of NPAHs and PAHs in Hanoi

Site	(1-NP)/(Pyr)[a]			(6-NBaP)/(BaP)[a]	(7-NBaA)/(BaA)[a]
	Summer	Winter	Average	Average	Average
I	0.066 ± 0.075	0.025 ± 0.035	0.045 ± 0.055	0.004 ± 0.005	0.096 ± 0.158
T	0.145 ± 0.22	0.075 ± 0.098	0.110 ± 0.159	0.008 ± 0.005	0.065 ± 0.067

[a] All data show mean ± SD.

1-NP and 7-NBaA have been recognized as primary sources from automobile exhausts. The [1-NP]/[Pyr] concentration ratios in particulate phase at sites I and T (0.066 and 0.145) in summer were higher than those in winter (0.025 and 0.075), respectively. This fact may be due to higher temperature in summer which contributes to decrease of Pyr proportion in the gas phase. Although Pyr is semi-volatile and our sampling campaign measured PAHs and NPAHs only in the particle phase, we could estimate the [1-NP]/[Pyr] ratio in the total gas/particle phase based on several reports (35,37). The highest value of [1-NP]/[Pyr] ratio (0.032) (in total gas/particle phase) appeared at site T in summer, and was nearer to the ratio for automobile exhausts in our previous studies (29,34). This indicates also that the largest contributors at site T in summer were motor vehicle engines. The lowest ratio (0.006) occurred at site I in winter. This value is close to the ratio at several cities, where the main contributor was coal combustion (29,38), and suggests that site I is near a place where coal is burned. According to the report from the Hanoi center for Environmental and Natural Resources Monitoring and Analysis (25), the total coal consumption for domestic cooking in Khuong Dinh ward (which is near sampling site I) was highest (0.58 ton/day) compared with other wards in the same Thanh Xuan district. Furthermore, coal consumption in the Thuong Dinh industrial area, which has rubber, soap powder, fabric, and vacuum flask factories and which is close to site I, was about 9.6 ton/day, and was the largest consumption in the inner Hanoi city. This might explain why [1-NP]/[Pyr] ratio was smaller at site I than that at site T. The [7NBaA]/[BaA] ratios in the present study were 0.096 and 0.065 at sites I and T, respectively, near the ratio for automobile exhausts (0.14), but far from the ratio for coal-smoke combustion (< 0.001) (29,33,34), suggesting that the main contributors to PAHs and NPAHs emissions in Hanoi were motor vehicle engines.

Comparison of PAH and NPAH Levels between Hanoi (a Motorbike City) and Other Cities

There are no specific regulations for the emission of PAHs and NPAHs from motorbikes in Vietnam. First, we compared the PAHs and NPAHs concentrations between Hanoi and other Asian cities including typical automobile

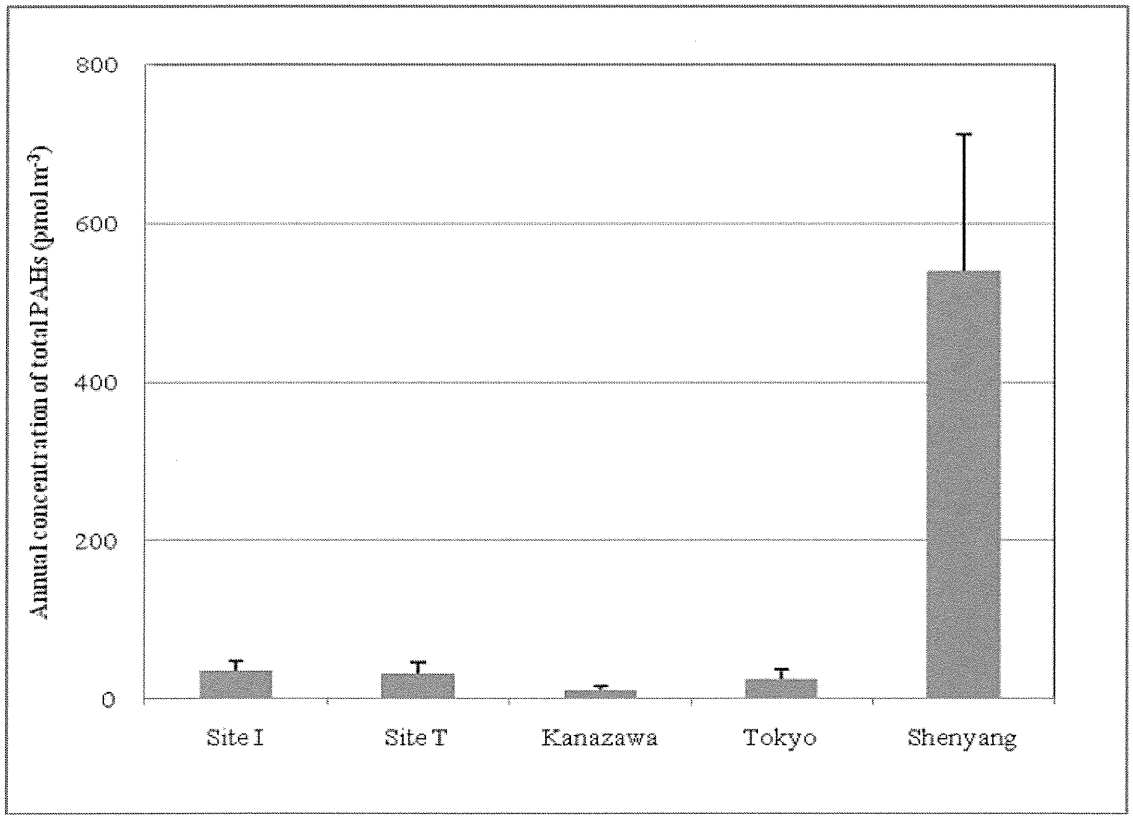

Figure 1: Annual concentrations of total PAHs in Hanoi and other cities. Total PAHs = (Flu) + (Pyr) + (B*a*A) + (Chr) + (B*b*F) + (B*k*F) + (B*a*P) + (B*ghi*Pe) + (IDP); Bars show standard deviations of the average. Data of Kanazawa, Tokyo and Shenyang cited from our previous reports (30, 34) were used for the calculation.

cities in Japan (Tokyo and Kanazawa) and a typical coal-burning city in China (Shenyang) (29,33). The total mean concentrations of 9 PAHs were 35.6 pmol m^{-3} at site I and 32.4 pmol m^{-3} at site T. These values were slightly higher than the value at Tokyo and 3.5 times higher than the value at Kanazawa, but only 6% of the value at Shenyang (Figure 1). The high value in Shenyang is due to coal burning, which releases large amounts of PAHs (42). The total average concentration of 5 NPAHs (9-NA, 1-NP, 7-NBaA, 6-NBaP, and 1-NPer) in Hanoi (536 ± 241 fmol m^{-3} at site I and 645 ± 237 fmol m^{-3} at site T) was 6 and 3 times higher than the values in Kanazawa and Tokyo, respectively, but only 16% of the value in Shenyang (Figure 2).

Next, we compared the PAH composition in Hanoi with the PAH compositions in other cities (Figure 3). The ratio of 4-ring/6-ring PAHs ([Flu + Pyr + B*a*A + Chr]/[B*ghi*Pe + IDP]) was lower in summer than that in winter in all cities. The higher temperature and stronger sunlight in summer are considered as a possible reason for the lower 4-ring/6-ring PAHs ratio. The distribution percentage of 4-ring PAHs, which are semi-volatile in the gas phase in the atmosphere, is increased with the increase in the temperature. Moreover,

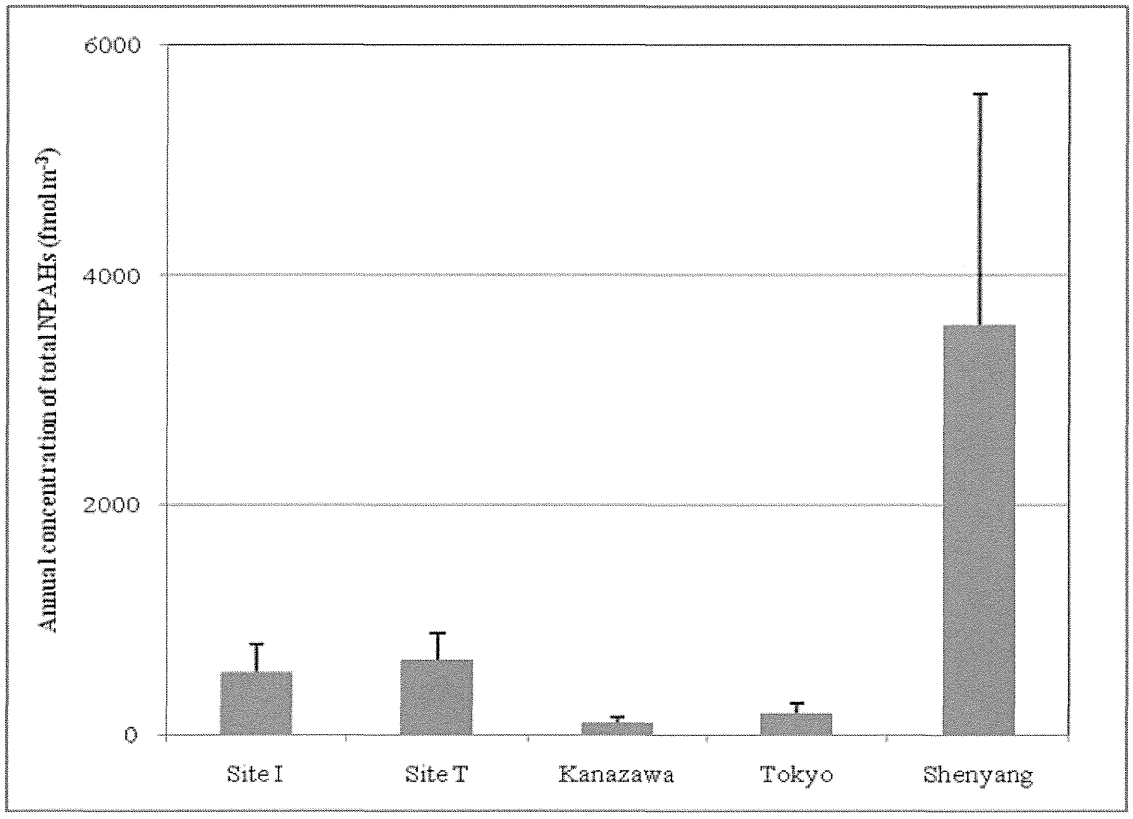

Figure 2: Annual concentrations of total NPAHs in Hanoi and other cities. Total NPAHs = (9-NA) + (1-NP) + (7-NB*a*A) + (6-NB*a*P) + (1-NPer); Bars show standard deviations of the average. Data of Kanazawa, Tokyo and Shenyang cited from our previous reports (30, 34) were used for the calculation.

degradation of lower molecular weight PAHs is accelerated by the radiation of sunlight. A large fraction of 4-ring PAHs such as Flu and Pyr from automobiles has been found in some previous studies (19,43). However, the proportion (%) of PAHs with six rings at both sites in Hanoi was higher than that at automobile cities (Kanazawa and Tokyo) and also much higher than that at Shenyang, where the main contributor was coal combustion. The differences of 6-ring PAHs proportion between Hanoi and other cities were about 8–28% in summer and 10–28% in winter. Many studies found that large PAHs such as B*ghi*Pe and Coronene (Cor) are the most abundant PAHs emitted from non catalyzed engines and light-duty gasoline engines (12,23,43,44). As mentioned above, one of specific characteristics of traffic situation in Hanoi city is the large volume of motorbikes without catalyst converters. Motorbikes account for around 90% of the total means of travel in Hanoi, and even 95–96% in many roads in the center of city. Furthermore, most of light duty and heavy duty vehicles in Hanoi were old and generally poorly maintained (45). A possible reason for the above composition differences is that motorbikes without catalytic converters and light-duty gasoline engines may emit larger amounts

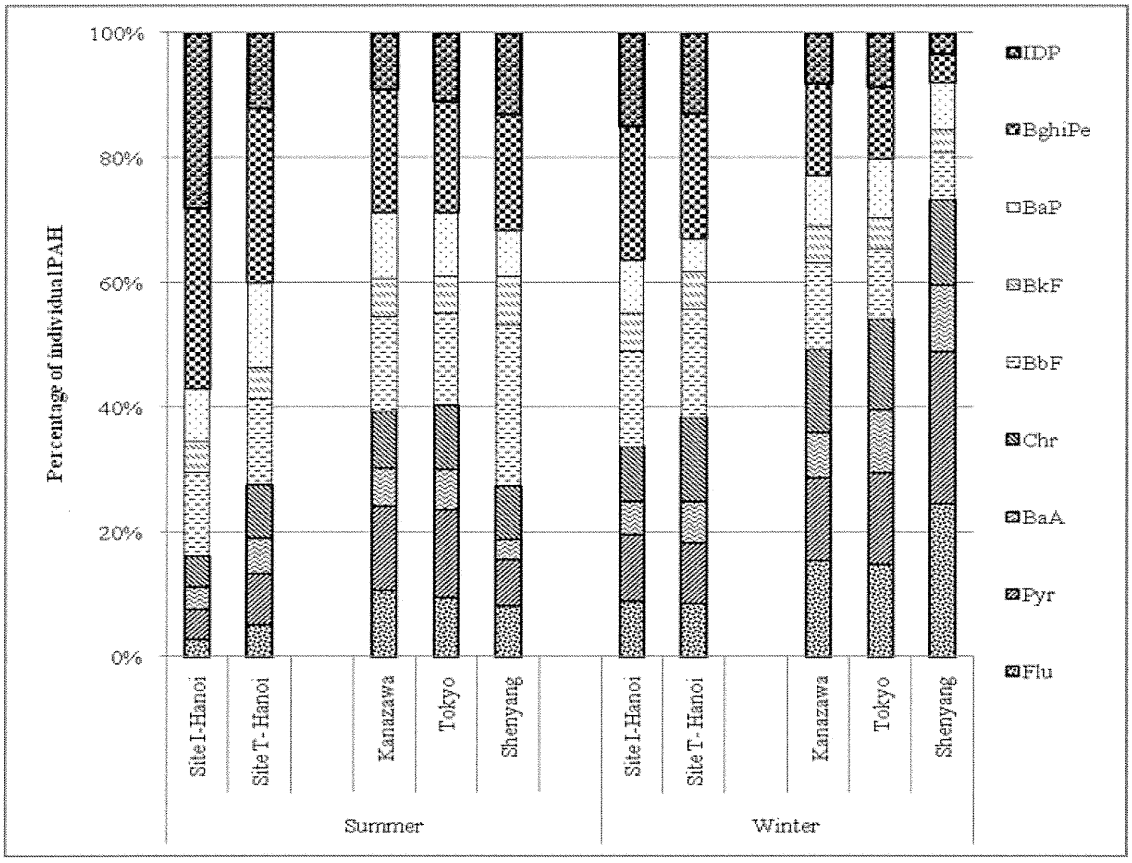

Figure 3: Comparison of PAHs distribution between Hanoi and other cities. Four-ring PAHs = (Flu) + (Pyr) + (B*a*A) + (Chr); 5-ring PAHs = (B*b*F) + (B*k*F) + (B*a*P); 6-ring PAHs = (B*ghi*Pe) + (IDP). Data of Kanazawa, Tokyo and Shenyang cited from our previous reports (30, 34) were used for the calculation.

of 6-ring PAHs than those of PAHs having 4 and 5 rings. The analysis of PAHs and NPAHs in exhausts directly collected from motorbike engines with and without catalytic converters might provide more accurate estimates of the contribution of motorbikes in Hanoi, Vietnam.

NPAHs distribution was also compared between Hanoi and the other cities in East Asia (Figure 4). In Hanoi, 7-NB*a*A was the second largest NPAH at both sites in both seasons, except for site T in winter. Although the proportion (%) of 4-ring NPAHs (1-NP + 7-NB*a*A) was not significantly different between Hanoi and other cities, the contribution of 7-NB*a*A to the total 5 NPAHs at both sites of Hanoi in both seasons was about 2–7 times higher than those in Kanazawa and Tokyo and much larger than those in Shenyang. The maximum difference for 7-NB*a*A was observed between site I and Shenyang. The proportion of 7-NBaA at site I was about 1/3 and 1/5 higher than that of Shenyang in summer and winter, respectively. Moreover, the level of 9-NA was higher in winter than in summer at all sites. This compound attained the highest concentration at all sites in winter and appeared significantly higher in

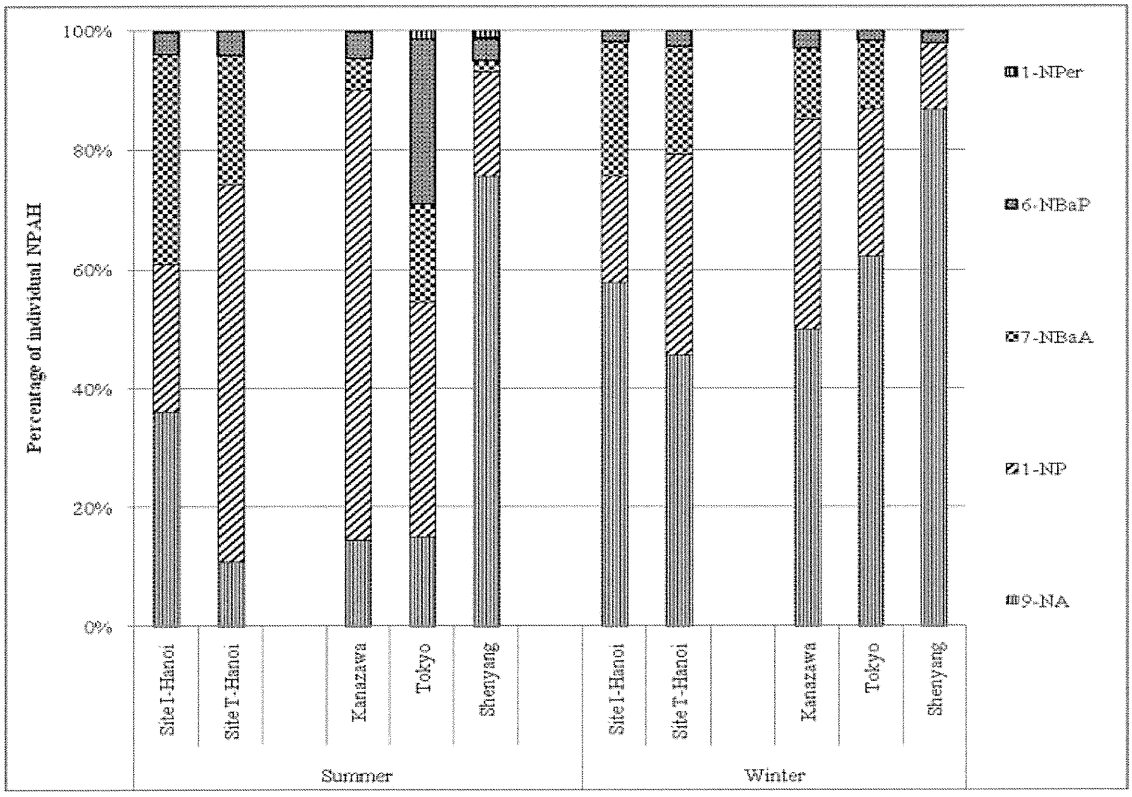

Figure 4: Comparison of NPAHs distribution between Hanoi and other cities. Three-ring NPAHs = (2-NA); 4-ring NPAHs = (1-NP) + (7-NB*a*A); 5-ring NPAHs = (6-NB*a*P) + (1-NPer). Data of Kanazawa, Tokyo and Shenyang cited from our previous reports (30, 34) were used for the calculation.

Shenyang in both seasons (75% in summer and 86% in winter). The concentration ratios of NPAHs with their parent PAHs in the four cities are compared in Figure 5. The mean values in Hanoi were taken from the average values at sites I and T. The mean ratio of [1-NP]/[Pyr] in Hanoi was 0.078, slightly larger than those of Kanazawa (0.055) and Tokyo (0.031). Meanwhile, this ratio was much smaller in Shenyang (0.017), a typical coal-burning city. The mean ratio of [7-NB*a*A]/[B*a*A] in Hanoi was 0.08, followed by those of Tokyo (0.026) and Kanazawa (0.016). The smallest value was observed in Shenyang (0.004). The concentration ratio of [6-NB*a*P]/[B*a*P] was highest in Kanazawa (0.008), followed by those of Hanoi (0.006) and Tokyo (0.0044), while it was the smallest (0.0026) in Shenyang. These facts coincide with previous studies that the [NPAH]/[PAH] ratio increases with rising combustion temperature (29). The combustion temperature in automobile and motorbike engines are around 2,700–3,000°C while the combustion temperature in coal burning systems such as coal stoves is 900–1,100°C. Thus, the concentration ratio of NPAH to the parent PAH in Shenyang was considerably smaller than that in Hanoi city. Moreover, it is interesting that this ratio was slightly larger in motorbike cities than in automobile cities, except for the [6-NB*a*P]/[B*a*P] ratio.

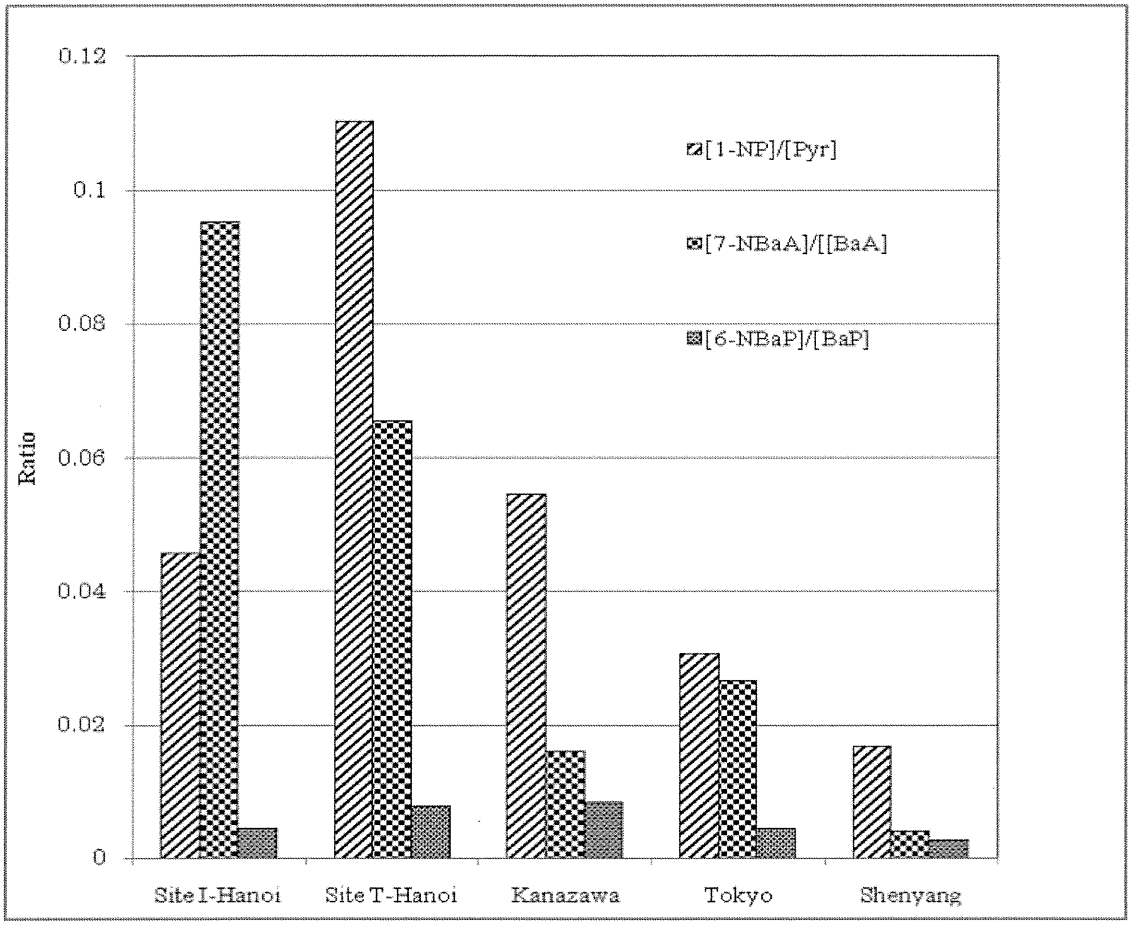

Figure 5: Comparison of (NPAH)/(PAH) ratios between Hanoi and other cities. Data of Kanazawa, Tokyo and Shenyang cited from our previous reports (30, 34) were used for the calculation.

These ratios might be useful markers for estimating the motorbike contribution to atmospheric PAHs and NPAHs. Figure 5 suggested that, in general, [NPAH]/[PAH] ratio was in the order: motorbikes cities > automobile cities > coal burning cities.

CONCLUSIONS

This is the first comprehensive report on atmospheric PAH and NPAH distributions in Hanoi, a typical motorbike city in the world. The average summer and winter concentrations of 10 PAHs having 4–6 rings were higher than those in Tokyo and Kanazawa, which are typical automobile cities but much lower than those in Shenyang, a typical coal-burning city. The predominant PAHs in Hanoi were 6-ring PAHs, B*ghi*Pe and IDP. The contribution of the 6-ring PAHs was much higher at site I (57% and 40%) than that at site T (36% and 33%) in summer and winter, respectively. This level was significantly higher than that

in automobile and coal-burning cities such as described above. The molecular diagnostic ratios of [6-NBaP]/[BaP], [7-NBaA]/[BaA] and [1-NP]/[Pyr] indicate the major contributors were motorbikes at site T and motorbikes and factories at site I. 1-NP appeared as the most abundant NPAH at site T while 9-NA was the predominant NPAH at site I. Although 7-NB*a*A was the second most abundant NPAH among five most abundant NPAHs, the contribution of 7-NB*a*A in Hanoi was much higher than it was in other cities. The concentration ratios of NPAH and PAH, [1-NP]/[Pyr], and [7-NB*a*A]/[B*a*A], in Hanoi were considerably higher than those in Tokyo and Kanazawa and much higher than those in Shenyang, whereas the [6-NBaP]/[BaP] ratio was slightly smaller than it was in other cities. These differences between Hanoi and the other cities may be due to the high number of motorbikes without catalytic converters. We are currently investigating this possibility by collecting particulates directly from motorbike exhausts in Hanoi city.

REFERENCES

1. IARC. Some Drinking-water Disinfectants and Contaminants, including Arsenic, Lyon, in *IARC Monographs on the Evaluation of Carcinogenic Risks to Humans* Vol. 84. (IARC, 2004), 39–267.

2. Chetwittayachan, T., D. Shimazaki, and K. Yamamoto. "A Comparison of Temporal Variation of Particle-bound Polycyclic Aromatic Hydrocarbons (PAHs) Concentration in Different Urban Environments: Tokyo, Japan, and Bangkok, Thailand." *Atmospheric Environment* 36 (2002): 2027–37.

3. Greenberg, A. and F. Darck. "Polycyclic Aromatic Hydrocarbons in New Jersey: A Comparison of Winter and Summer Concentrations over a Two-Year Period." *Atmospheric Environment* 19 (1985): 1325–39.

4. Baek, S. O., R. A. Field, M. E. Goldstone, P. W. Kirk, J. N. Lester, and R. Perry. "A Review of Atmospheric Polycyclic Aromatic Hydrocarbons: Source, Fate and Behavior." *Water, Air, and Soil Pollution* 60 (1991): 279–300.

5. Brorström-Lundén, E. "Monitoring Ambient Quality for Health Impact Assessment." WHO Regional Publications, European Series, No. 85 (1999).

6. Finlayson-Pitts, B. J. and J. N. Pitts. *Atmospheric Chemistry*. (New York: Wiley-Interscience, 1986).

7. Bi, X., G. Sheng, P. Peng, Y. Chen, Z. Zhang, and J. Fu. "Distribution of Particulate- and Vapor-Phase n-alkanes and Polycyclic Aromatic Hydrocarbons in Urban Atmosphere of Guangzhou, China." *Atmospheric Environment* 37 (2003): 289–98.

8. Chang, K. F, G. C. Fang, J. C. Chen, and Y. S. Wu. "Atmospheric Polycyclic Aromatic Hydrocarbons (PAHs) in Asia: A Review from 1999 to 2004." *Environmental Pollution* 142 (2006): 388–96.

9. Yasmin, W. F. T., K. Takeda, and H. Sakugawa. "Polycyclic Aromatic Hydrocarbons (PAHs) Associated with Atmospheric Particles in Higashi Hiroshima, Japan: Influence of Meteorological Conditions and Seasonal Variations." *Atmospheric Research* 88 (2007): 224–33.

10. Perrini, G., M. Tomasello, V. Librando, and Z. Minniti. "Nitrated Polycyclic Aromatic Hydrocarbons in the Environment: Formation, Occurrences and Analysis." *Journal of Analytical, Environmental and Cultural Heritage Chemistry* 95 (2005): 567–77.

11. Albinet, A., E. Leoz-Garziandia, H. Budzinski, and E. ViIlenave. "Polycyclic Aromatic Hydrocarbons (PAHs), Nitrated PAHs and Oxygenated PAHs in Ambient Air of the Marseilles Area (South of France): Concentrations and Sources." *Science of the Total Environment* 384 (2007): 280–92.

12. Caricchia, A. M., S. Chiavarini, and M. Pezza. "Polycyclic Aromatic Hydrocarbons in the Urban Atmospheric Particulate Matter in the City of Naples (Italy)." *Atmospheric Environment* 33 (1999): 3731–8.

13. Hsu, I. and T. Pen. "A Comparison Study on Motorcycle Traffic Development in some Asian Countries–Case of Taiwan, Malaysia and Vietnam." Final Report, The Eastern Asia Society for Transportation Studies (EASTS), International Cooperative Research Activity (2003).

14. Yang, H. H., S. M. Chien, M. R. Chao, and C. C. Lin. "Particle Size Distribution of Polycyclic Aromatic Hydrocarbons in Motorcycle Exhaust Emissions." *Journal of Hazardous Materials* B125 (2005): 154–9.

15. Lin, C. W., S. J. Lu, and K. S. Lin. "Test Emission Characteristics of Motorcycles in Central Taiwan." *Science of the Total Environment* 368 (2006): 435–43.

16. Spezzano, P., P. Picini, D. Cataldi, F. Messale, and C. Manni. "Particle- and Gas-Phase Emissions of Polycyclic Aromatic Hydrocarbons from Two-Stroke, 50-cm^3 Mopeds." *Atmospheric Environment* 42 (2008): 4332–44.

17. Spezzano, P., P. Picini, and D. Cataldi. "Gas- and Particle-phase Distribution of Polycyclic Aromatic Hydrocarbons in Two-Stroke, 50-cm^3 Moped Emissions." *Atmospheric Environment* 43 (2009): 539–45.

18. Mishima, K. "Empirical Issues and Theoretical Problems on the Motorcycle Industry in Southeast Asia (Japanese)." *Kaigai-jijo-kenkyu* 36, no. 1 (2005): 29–59.

19. Abrantes, R., J. Assunção, and C. Pesquero. "Emission of Polycyclic Aromatic Hydrocarbons from Light-Duty Diesel Vehicles Exhaust." *Atmospheric Environment* 38 (2004): 1631–40.

20. Murahashi, T., M. Miyazaki, R. Kakizawa, Y. Yamagishi, M. Kitamura, and K. Hayakawa. "Diurnal Concentration of 1,3-, 1,6-, 1,8-dinitropyrenes, 1-nitropyrene and Benzo[*a*]pyrene in Air in Downtown Kanazawa and the Contribution of Diesel-Engine Vehicles." *Japanese Journal of Toxicology and Environmental Health* 41 (1995): 328–33.

21. Zanini, G., M. Bericoa, F. Monforti, L. Vitali, S. Zambonelli, S. Chiavarini, T. Georgiadis, and M. Nardino. "Concentration Measurement in a Road Tunnel as a Method to Assess "Real-World" Vehicles Exhaust Emissions." *Atmospheric Environment* 40 (2006): 1242–54.

22. Chen, S. J., W. J. Lee, W. C. Chien, and S. H. Liao. "Characterization of PAHs in the Exhaust of a Gasoline-Powered Engine." *Journal of Aerosol Science* 29, Suppl. I (1998): 355–6.

23. Riddle, S. G., C. A. Jakober, M. A. Robert, T. M. Cahill, M. J. Charles, and M. J. Kleeman. "Large PAHs Detected in Fine Particulate Matter Emitted from Light-Duty Gasoline Vehicles." *Atmospheric Environment* 41 (2007): 8658–68.

24. Hien, P. D., V. T. Bac, H. C. Tham, D. D. Nhan, and L. D. Vinh. "Influence of Meteorological Conditions on PM2.5 and PM2.5-10 Concentrations during the Monsoon Season in Hanoi, Vietnam." *Atmospheric Environment* 36 (2002): 3473–84.

25. Hung, N. T. "Urban Air Quality Modeling and Management in Hanoi, Vietnam." PhD Thesis, Aarhus University, National Environmental Research Institute, Denmark (2010).

26. Vietnamese Ministry of Industry, Institute for Industry Policy and Strategy. "Master Plan for the Development of Vietnam's Motorcycle Industry in the Period of 2006–2015, with a Vision to 2020." (2007). http://www.vdf.org.vn/DOC/2007/MMP_ApprovedNov07E.pdf, Accessed May 28, 2012.

27. Engineering and Consulting Firms Association, Japan Nippon Koei Co., Ltd. *Preliminary Study on Traffic Control Center in Hanoi.* Report. (2011). http://www.ecfa.org.jp/japanese/act-pf_jka/H22/koei_hanoi22.pdf, Accessed May 28, 2012.

28. Vietnam Environment Administration. *Annual Report on Environmental Pollution*. (2010). http://vea.gov.vn, Accessed on December 27, 2011.

29. Tang, N., T. Hattori, R. Taga, K. Igarashi, X. Yang, K. Tamura, H. Kakimoto, V. F. Mishukov, A. Toriba, R. Kizu, and K. Hayakawa. "Polycyclic Aromatic Hydrocarbons and Nitropolycyclic Aromatic Hydrocarbons in Urban Air Particulates and Their Relationship to Emission Sources in the Pan–Japan Sea Countries." *Atmospheric Environment* 39 (2005): 5817–26.

30. Liu, L., Y. Liu, J. Lin, N. Tang, K. Hayakawa, and T. Maeda. "Development of Analytical Methods for Polycyclic Aromatic Hydrocarbons (PAHs) for Airborne Particulates: A Review." *Journal of Environmental Sciences* 19 (2007): 1–11.

31. Tsakas, M. P., I. E. Sitaras, and P. A. Siskos. "Nitro Polycyclic Aromatic Hydrocarbons in Atmospheric Particulate Matter of Athens, Greece." *Chemistry and Ecology* 26 (2010): 251–61.

32. Tang, N., H. Hama, T. Kameda, A. Toriba, and K. Hayakawa. "Change of Atmospheric Concentrations and Source of Benzo[a]pyrene and 6-nitrobenzo[a]pyrene in Kanazawa, a Typical Local City in Japan during 1999 and 2010." *Environmental Forensics: Proceedings of the 2011 INEF Conference* (2012).

33. Hayakawa, K., N. Tang, T. Kameda, and A. Toriba. "Atmospheric Behaviors of Polycyclic Aromatic Hydrocarbons and Nitropolycyclic Aromatic Hydrocarbons in East Asia." *Asian Journal of Atmospheric Environment* 1 (2007): 19–27.

34. Hayakawa, K. "Atmospheric Pollution and its Countermeasure in East Asia from the Viewpoint of Polycyclic Aromatic Hydrocarbons." *Journal of Health Science* 55 (2009): 870–8.

35. Mugica, V., S. Hernández, M. Torres, and R. García. "Seasonal Variation of Polycyclic Aromatic Hydrocarbon Exposure Levels in Mexico City." *Journal of the Air and Waste Management Association* 60, no. 5 (2010): 548–55.

36. Albaiges, J., J. M. Bayona, P. Fernandez, J. Grimalt, A. Rosell, and R. Simo. "Vapor-Particle Partitioning of Hydrocarbons in Western Mediterranean Urban and Marine Atmospheres." *Microchimica Acta* 104, no. 11 (1991): 13–27.

37. Araki, U., N. Tang, M. Ohno, T. Kameda, A. Toriba, and K. Hayakawa. "Analysis of Atmospheric Polycyclic Aromatic Hydrocarbons and Nitropolycyclic Aromatic Hydrocarbons in Gas/Particle Phases Separately Collected by a High Volume Air Sampler Equipped with a Column Packed with XAD-4 Resin." *Journal of Health Science* 55, no. 1 (2009): 77–85.

38. Tang, N., Y. Araki, K. Tamura, L. Dong, X. Zhang, Q. Liu, R. Ji, T. Kameda, A. Toriba, and K. Hayakawa. "Distribution and Source of Atmospheric Polycyclic Aromatic Hydrocarbons and Nitropolycyclic Aromatic Hydrocarbons in Tieling City, Liaoning Province, a Typical Local City in Northeast China." *Asian Journal of Atmospheric Environment* 3 (2009): 52–8.

39. Kavouras, I. G., P. Koutrakis, M. Tsapakis, E. Lagoudaki, E. G. Stephanou, D. V. Baer, and P. Oyola. "Source Apportionment of Urban Particulate Aliphatic and Polynuclear Aromatic Hydrocarbons (PAHs) using Multivariate Methods." *Environmental Science and Technology* 35 (2001): 2288–94.

40. Manoli, E., A. Kouras, and C. Samara. "Profile Analysis of Ambient and Source Emitted Particle-Bound Polycyclic Aromatic Hydrocarbons from three Sites in Northern Greece." *Chemosphere* 56 (2004): 867–78.

41. Hien, T. T., P. P. Nam, S. Yasuhiro, T. Kameda, T. Norimichi, and B. Hiroshi. "Comparison of Particle-Phase Polycyclic Aromatic Hydrocarbons and Their Variability Causes in the Ambient Air in Ho Chi Minh City, Vietnam and in Osaka, Japan, during 2005–2006." *Science of the Total Environment* 382 (2007): 70–81.

42. Yang, X. Y., Y. Okada, N. Tang, S. Matsugana, K. Tamura, J. M. Lin, T. Kameda, A. Toriba, and K. Hayakawa. "Long-range Transport of Polycyclic Aromatic Hydrocarbon from China to Japan." *Atmospheric Environment* 41 (2007): 2710–18.

43. Rogge, W. F., L. M. Hildemann, M. A. Mazurek, and G. R. Cass. "Sources of Fine Organic Aerosol 2: Noncatalyst and Catalyst-equipped Automobiles and Heavy-duty Diesel Trucks." *Environmental Science and Technology* 27 (1993): 636–51.

44. Ravindra, K., R. Sokhi, and R. V. Griekén. "Atmospheric Polycyclic Aromatic Hydrocarbons: Source Attribution, Emission Factors and Regulation." *Atmospheric Environment* 42 (2008): 2895–2921.

45. Thuy, T. T. B. "Vehicular Air Pollution Management in Hanoi City, Vietnam." *Proceedings of Pre-event at Better Air Quality 2006 Workshop*, Yogyakarta, India (2006): 27–41.

46. Miller-Schulze, J. P., M. Paulsen, A. Toriba, N. Tang, K. Hayakawa, K. Tamura, L. Dong, Z. Zhang, and C. D. Simpson. "Exposures to Particulate Air Pollution and Nitro-polycyclic Aromatic Hydrocarbons among Taxi Drivers in Shenyang, China." *Environmental Science and Technology* 44 (2010): 216–21.

47. Feilberg, A., M. W. B. Poulsen, T. Nielsen, and H. Skov. "Occurrence and Sources of Particulate Nitro-Polycyclic Aromatic Hydrocarbons in Ambient Air in Denmark." *Atmospheric Environment* 35 (2001): 353–66.

48. Harrison, R. M., D. J. T. Smith, and L. Luhana. "Source Apportionment of Atmospheric Polycyclic Aromatic Hydrocarbons Collected from an urban location in Birmingham." *Environmental Science and Technology* 30 (1996): 825–32.

49. Hayakawa, K., N. Tang, K. Akutsu, T. Murahashi, H. Kakimoto, R. Kizu, and A. Toriba. "Comparison of Polycyclic Aromatic Hydrocarbons and Nitropolycyclic Aromatic Hydrocarbons in Airborne Particulates Collected in Downtown and Suburban Kanazawa, Japan." *Atmospheric Environment* 36 (2002): 5535–41.

50. Masao Kishida, M., K. Imamura, N. Takenaka, Y. Maeda, P. H. Viet, and H. Bandow. "Concentrations of Atmospheric Polycyclic Aromatic Hydrocarbons in Particulate Matter and the Gaseous Phase at Roadside Sites in Hanoi, Vietnam." *Bulletin of Environmental Contamination and Toxicology* 81 (2008): 174–9.

Biological Sciences in Space, Vol.26, 26-31, 2012

Original Paper

Determination of Calcium Sensing Receptor in the Scales of Goldfish and Induction of Its mRNA Expression by Acceleration Loading

Makiko Kakikawa[1], Tatsuki Yamamoto[2], Vishwajit S. Chowdhury[3], Yusuke Satoh[4], Kei-ichiro Kitamura[4], Toshio Sekiguchi[2], Hisayuki Funahashi[5], Katsunori Omori[6], Masato Endo[7], Sachiko Yano[8], Sotoshi Yamada[1], Kazuichi Hayakawa[9], Atsuhiko Chiba[10], Ajai K. Srivastav[11], Kenichi Ijiri[12], Azusa Seki[13], Atsuhiko Hattori[14] and Nobuo Suzuki[2]*

[1]Institute of Nature and Environmental Technology, Kanazawa University, Kakuma, Ishikawa 920-1192, Japan
[2]Noto Marine Laboratory, Institute of Nature and Environmental Technology, Kanazawa University, Housu-gun, Ishikawa 927-0553, Japan
[3]International Education Center, Faculty of Agriculture, Kyushu University, Fukuoka 812-8581, Japan
[4]Department of Clinical Laboratory Science, Graduate School of Medical Science, Kanazawa University, Kodatsuno, Ishikawa 920-0942, Japan
[5]Department of Anatomy, Showa University School of Medicine, Shinagawa-ku, Tokyo 142-8555, Japan
[6]Faculty of Economics, Asia University, Musashino, Tokyo 180-8629, Japan
[7]Graduate School of Marine Science and Technology, Tokyo University of Marine Science and Technology, Minato-ku, Tokyo 108-8477, Japan
[8]Japan Aerospace Exploration Agency, Tsukuba, Ibaraki 305-8505, Japan
[9]Faculty of Pharmaceutical Sciences, Institute of Medical, Pharmaceutical and Health Sciences, Kanazawa University, Kakuma, Ishikawa 920-1192, Japan
[10]Department of Materials and Life Sciences, Sophia University, Tokyo 102-8554, Japan
[11]Department of Zoology, University of Gorakhpur, Gorakhpur 273009, India
[12]Radioisotope Center, The University of Tokyo, Bunkyo-ku, Tokyo 113-0032, Japan
[13]HAMRI Co., Ltd., Koga, Ibaraki 306-0101, Japan
[14]Department of Biology, College of Liberal Arts and Sciences, Tokyo Medical and Dental University, Ichikawa, Chiba 272-0827, Japan

Received: November 5, 2012; Accepted: November 21, 2012

*To whom correspondence should be addressed:
Tel.: +81-(0)768-74-1151; Fax: +81-(0)768-74-1644;
E-mail: nobuos@staff.kanazawa-u.ac.jp

Abstract

It is known that the teleost scale regenerates after being removed. We previously reported that the osteogenesis in regenerating scales was very similar to that in calvarial bone, which suggests that regenerating scale can be used as a model for osteogenesis. In the present study, we determine calcium sensing receptor (CaSR) cDNA from the regenerating scales of goldfish. The determined partial sequence was coded as a 258-amino acid protein. The amino acid identity of this receptor to teteost CaSRs is 89 to 96%, lizard CaSR is 82%, and mammalian CaSR is 83 to 84%. These results indicate that CaSR is highly conserved in fish, lizard and mammals. Then, to examine the role of CaSR in bone metabolism, effect of acceleration loading (3 *G*) by vibration on the expression of CaSR mRNA in the regenerating scales of goldfish was investigated. We found that CaSR mRNA expression increased after acceleration loading by vibration in the regenerating scales. Significant difference between control and treatment group was observed at 6 and 24 h of incubation. Our cloned CaSR appears to act for the metabolism of bone in the regenerating scales. This is the first demonstration, to our knowledge, of an effect of hyper-loading on the induction of CaSR mRNA expression of hard tissues. ©2012 Jpn. Soc. Biol. Sci. Space; doi: 10.2187/bss.26.26

***Key words*: CaSR, regenerating scale, osteoblasts, acceleration loading by vibration**

Introduction

The calcium sensing receptor (CaSR), a G protein-coupled receptor that responds to extracellular calcium, was first determined from bovine parathyroid gland (Brown *et al.*, 1993). Therefore, it is considered that CaSR plays a central role in controlling systemic calcium homeostasis, predominately through its effects on the regulation of parathyroid hormone (PTH) secretion by the parathyroid glands and on urinary calcium excretion by the kidney (Brown *et al.*, 1993; Brown and MacLeod, 2001). However, it was reported that CaSR located in many tissues and was involved in cell proliferation differentiation, and apoptosis (Hofer and Brown, 2003; Kwak *et al.*, 2005; Smajilovic *et al.*, 2006; Xu *et al.*, 2012). In the MC3T3-E1 cells, an osteoblast-like cell line, high extracellular calcium stimulated cell proliferation (Yamaguchi *et al.*, 1998). As CaSR was expressed in the MC3T3-E1 cells, calcium signaling is seems to transmit *via* CaSR in the MC3T3-E1 cells (Yamaguchi *et al.*, 1998; Godwin and Soltoff, 2002). Therefore, it is considered that CaSR regulates osteoblastic functions such as bone development and mineralization (Theman and Collins, 2009; Dvorak-Ewell *et al.*, 2011). On the other hand, the bone matrix plays an important role for response to

physical stimuli (Harter *et al.*, 1995; Owan *et al.*, 1997; Hoffler *et al.*, 2006). In addition, Sun *et al.* (2012) reported that mechanical stretch induced calcium efflux from bone matrix and stimulated osteoblasts. As few techniques for culture system of bone cells including bone matrix have been developed, the function of CaSR under physical stimuli has not elucidated yet.

The teleost scale is a calcified tissue that contains osteoblasts, osteoclasts, and the bone matrix of two layers (bony layer: a thin, well-calcified external layer; a fibrillary layer: a thick, partially calcified layer) (Bereiter-Hahn and Zylberberg, 1993; Suzuki *et al.*, 2000; Yoshikubo *et al.*, 2005; Suzuki *et al.*, 2007; Ohira *et al.*, 2007). Furthermore, it is known that the teleost scale regenerates after being removed. In our previous study, we reported that the osteogenesis in regenerating scales was very similar to that in calvarial bone (Yoshikubo *et al.*, 2005). The response of osteoblasts to estrogen in regenerating scales was higher than that in developed normal scales (Yoshikubo *et al.*, 2005). Using the regenerating scales, we previously demonstrated that scale osteoblastic activity responses to low-loading (3 *G*) for 10 min by vibration increased (Suzuki *et al.*, 2009). As mammalian osteoblasts are activated by high-loading from 5 to 50 *G* (Gebken *et al.*, 1999; Saito *et al.*, 2003; Searby., 2005), the sensitivity to hyper-loading response in the regenerating scales possibly be high when compared with mammalian osteoblasts.

To examine the response of CaSR to hyper-loading, the cDNA of CaSR was cloned from the regenerating scales of goldfish and then the effect of acceleration loading by vibration on CaSR mRNA expression was investigated.

Materials and Methods

Animals

Both female and male goldfish (*Carassius auratus*) (20-30 g) were purchased from a commercial source (Higashikawa Fish Farm, Yamatokoriyama, Japan) and artificially fertilized. The hatched goldfish were kept in an aquarium at 25°C under a daily photoperiod cycle of 12 h light: 12 h darkness. Goldfish were provided *ad libitum* diets every morning. After having adequate size (around 15 g), the female goldfish were used in the experiment because we previously reported that the sensitivity for a calcemic hormone, such as estrogen and calcitonin, was higher in mature female than in mature male goldfish (Suzuki *et al.*, 2000). All experimental procedures were conducted in accordance with the Guide for the Care and Use of Laboratory Animals of Kanazawa University.

Cloning of CaSR from the scales of goldfish

Goldfish were anesthetized with ethyl 3-aminobenzoate, methanesulfonic acid salt (Sigma-Aldrich, Inc., MO, USA), and the developed normal scales on the body were then removed to allow the regeneration of scales. On day 14, goldfish were anesthetized again, and the regenerating scales were removed and kept at -80°C. Using the regenerating scales, CaSR was cloned.

Total RNAs were extracted from the regenerating scales of goldfish using a kit (Qiagen GmbH, Hilden, Germany). After cDNA synthesis (Qiagen GmbH), PCR was performed. The primers (5'-GGGATCAGYTTTGTTYTMTGCATC-3' and 5'-CCTCMACAGCYGARACAAACTT-3') were designed from conserved region among *Sparus aurata* (AJ289717), *Oreochromis niloticus* (XM_003446845), *Platichthys flesus* (FJ755006), *Salmo salar* (NM_001126231) and *Danio rerio* (XM_684005). Then, 5' rapid amplification of cDNA ends (RACE) were performed with nested primer (5'-CACCAGTAGGACACGATTGG-3' for 5'-RACE, bold and italic type in Fig.1) designed using the obtained sequence (BD SMART RACE cDNA amplification kit, BD Biosciences Clonetech, California, USA). The products were put into vector by TA cloning and then sequenced on ABI 310 sequencer (Applied Biosystems, California, USA). After determination of the sequences, the amino acid sequences were aligned using the clustal w program (Chenna *et al.*, 2003).

Acceleration-loading apparatus

Our loading apparatus has an acceleration-loading part and an acceleration-monitoring part. The detail was described in Suzuki *et al.* (2007). The acceleration-loading part, which consists of a sampling tube-loading stage and an aluminum plate with 2 vibration motors, is hung with 4 springs. Two vibration motors can provide a sinusoidal wave of acceleration ranging from 0.5 to 12 *G* in amplitude and from 8 to 50 Hz in frequency. The acceleration-monitoring part consists of a piezoelectric accelerometer, a charge amplifier, an A/D converter board, and a personal computer. A piezoelectric accelerometer, equipped on a sampling tube-loading stage, converts the loading acceleration into an analog electric signal. The signal was amplified with a charge amplifier (Yamco 4101, Yamaichi Electronics, Osaka, Japan) and transmitted *via* a 12-bit A/D converter board to a personal computer. Using software (LaBDAQ2000, Matsuyama Advan, Ehime, Japan), the PC allows us to monitor the real-time loading acceleration of the vibration. Therefore, we can load accurate gravity to the scales in a micro tube by confirming the amplitude and frequency of acceleration shown on the monitor screen.

Effect of acceleration loading by vibration on CaSR mRNA expression in the scales of goldfish

As described above, the regenerating scales were prepared and put into a 1.5 ml micro tube then 700 μl of Leibovitz's L-15 medium (Invitrogen, Grand Island, NY, USA) and a 1% penicillin-streptomycin mixture (ICN Biomedicals, Inc., OH, USA) were added. To fix the scales, a cotton ball (diameter 1 cm) was placed into a micro tube. The tube containing scales was loaded to 2 *G* acceleration by vibration for 10 min at room temperature. The loading times were determined according to our previous study (Suzuki *et al.*, 2007; Suzuki *et al.*, 2009). The lines on the left side were used as the treatment group, while those on the opposite side were used as the control group. In the loading, different parallel experiments using six goldfish were conducted. After loading for 10 min, the scales were incubated for 3-, 6-,

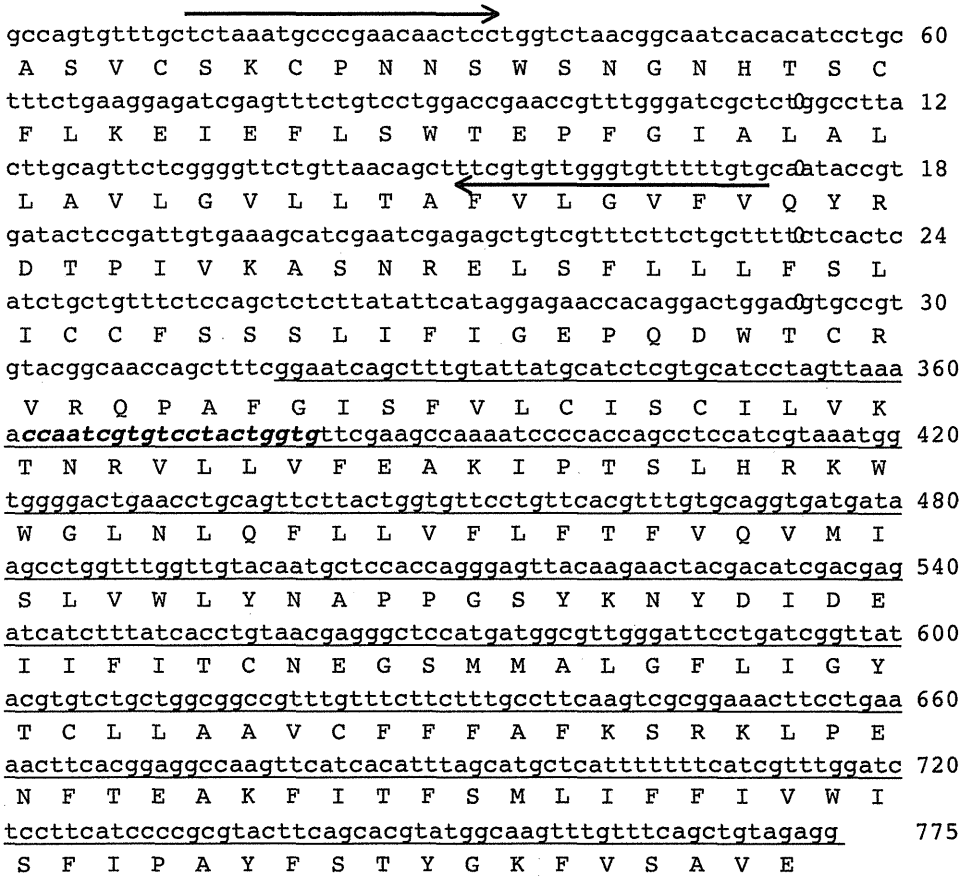

Fig. 1. Partial cDNA sequences of goldfish CaSR and the putative amino acid sequences. The underlined region is an obtained sequence by the first PCR. The CaSR mRNA expression in the scales of goldfish due to the effect of acceleration loading by vibration was examined using the primers shown by arrows. The primer for 5'-RACE indicated by bold and italic type. This data has been available under Genbank accession no. AB713518.

12-, and 24-h at 15°C. After incubation, the scales were frozen at -80°C until using for mRNA analysis. The loaded scales (3 *G*) were compared with unloaded (1 *G* control) scales.

After extraction of total RNAs, cDNA synthesis was performed using a kit (Qiagen GmbH). Gene-specific primers for CaSR (sense: 5'-TCTAAATGCCCGAACAACTCC-3'; antisense: 5'-CACAAAAACACCCAACACGA-3') (arrow in Fig.1) were design from the obtained sequence of goldfish CaSR. The amplification of β-actin cDNA was performed using a primer set (5'-CGAGCGTGGCTACAGCTTCA-3'; 5'-GCCCGTCAGGGAGCTCATAG-3') (Azuma *et al.*, 2007). The PCR amplification was analyzed by a real-time PCR apparatus (Mx3000p, Agilent Technologies, CA, USA) (Suzuki *et al.*, 2011). The annealing temperature for amplification of CaSR and β-actin was 60°C. The mRNA levels were normalized to the β-actin mRNA level.

Statistical analysis

All results are expressed as the means ± SEM (n = 6). The statistical significance was assessed by paired *t*-test.

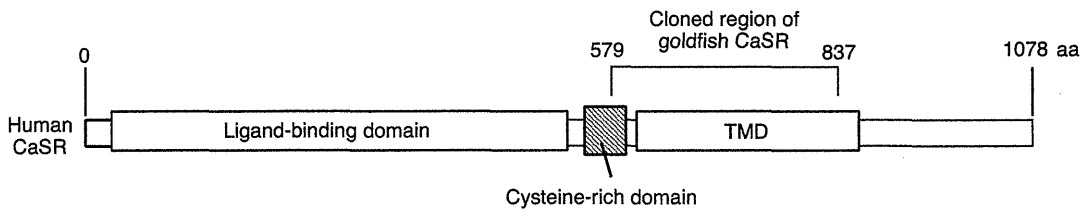

Fig.2. The molecular structure of human CaSR and the cloned region of goldfish CaSR. Human CaSR consists of 1078-amino acids (aa) and has ligand-binding domain (20-530 aa), cysteine-rich region (538-591 aa) and the transmembrane domain (622-860 aa).

```
goldfish    ASVCSKCPNNSWSNGNHTSCFLKEIEFLSWTEPFGIALALLAVLGVLLTAFVLGVFVQYRDTPIVKASNRELSFLLLFSLICCFSSSLIFIGEPQDWTCR
zebrafish   ASFCVKCPNNSWSNGNHTSCFLKQIEFLSWTEPFGIALALFAVLGVLLTAFVLGVFVQFRDTPIVKASNRELSFLLLFSLICCFSSSLIFIGEPQDWTCR
salmon      ASVCTKCPNDSWSNENHTSCFLKEIEFLSWTEPFGIALALCSVLGVFLTAFVMGVFIKFRNTPIVKATNRELSYLLLFSLICCFSSSLIFIGEPQDWTCR
lizard      ASACEKCAENFWSNENHTVCIPKQIEFLSWTEPFGIALTLFAILGIFLTSFVLGVFTRFRNTPIVKATNRELSYLLLFSLLCCFSSSLFFIGEPQDWNCR
pig         ASACDKCPDDFWSNENHTSCIAKEIEFLSWTEPFGIALTLFAVLGIFLTAFVLGVFIKFRNTPIVKATNRELSYLLLFSLLCCFSSSLFFIGEPQDWTCR
mouse       ASACDKCPDDFWSNENYTSCIAKEIEFLAWTEPFGIALTLFAVLGVFIKFRNTPIVKATNRELSYLLLFSLLCCFSSSLFFIGEPQDWTCR
human       ASACNKCPDDFWSNENHTSCIAKEIEFLSWTEPFGIALTLFAMLGIFLTAFVLGVFIKFRNTPIVKATNRELSYLLLFSLLCCFSSSLFFIGEPQDWTCR
            ** * **    *** * * *  * **** ********* *   **  ** ** ***   * ****** ***** ****** ******* ******** **

goldfish    VRQPAFGISFVLCISCILVKTNRVLLVFEAKIPTSLHRKWWGLNLQFLLVFLFTFVQVMISLVWLYNAPPGSYKNYDI-DEIIFITCNEGSMMALGFLIG
zebrafish   VRQPAFGISFVLCISCILVKTNRVLLVFEAKIPTSLHRKWWGLNLQFLLVFLFTFVQVMICVVWLYNAPPGSYKNYDI-DEIIFITCNEGSMMALGFLIG
salmon      LRQPAFGISFVLCISCILVKTNRVLLVFEAKIPTSLHRKWWGLNLQFLLVFLFTFVQVMICVVWLYNAPPASYRNHDI-DEIIFITCNEGSMMALGFLIG
lizard      LRQPAFGISFVLCISCILVKTNRVLLVFEAKIPTSLHRKWWGMNLQFLLVFLCTFVQIVICVIWLYTAPPSSFRNHELEDEIIFITCNEGSLMALGFLIG
pig         LRQPAFGISFVLCISCILVKTNRVLLVFEAKIPTSFHRKWWGLNLQFLLVFLCTFMQIVICAIWLYTAPPSSYRNHELEDEIIFITCHEGSLMALGFLIG
mouse       LRQPAFGISFVLCISCILVKTNRVLLVFEAKIPTSFHRKWWGLNLQFLLVFLCTFMQIVICIIWLYTAPPSSYRNHELEDEIIFITCHEGSLMALGSLIG
human       LRQPAFGISFVLCISCILVKTNRVLLVFEAKIPTSFHRKWWGLNLQFLLVFLCTFMQIVICVIWLYTAPPSSYRNQELEDEIIFITCHEGSLMALGFLIG
             ********************************** ****** ********* ** *  *   *** *** *  *    ******** *** **** ***

goldfish    YTCLLAAVCFFFAFKSRKLPENFTEAKFITFSMLIFFIVWISFIPAYFSTYGKFVSAVE
zebrafish   YTCLLAAICFFFAFKSRKLPENFTEAKFITFSMLIFFIVWISFIPAYFSTYGKFVSAVE
salmon      YTCLLAAICFFFAFKSRKLPENFTEAKFITFSMLIFFIVWISFIPAYFSTYGKFVSAVE
lizard      YTCLLAAICFFFAFKSRKLPENFNEAKFITFSMLIFFIVWISFIPAYASTYGKFVSAVE
pig         YTCLLAAICFFFAFKSRKLPENFNEAKFITFSMLIFFIVWISFIPAYASTYGKFVSAVE
mouse       YTCLLAAICFFFAFKSRKLPENFNEAKFITFSMLIFFIVWISFIPAYASTYGKFVSAVE
human       YTCLLAAICFFFAFKSRKLPENFNEAKFITFSMLIFFIVWISFIPAYASTYGKFVSAVE
            ******* *************** ********************** ***********
```

Fig. 3. Sequence alignment of goldfish CaSR with other CaSRs (zebrafish: XP_689097; salmon: NP_001119703; lizard: XP_003223807; pig: XP_003132690; mouse: AAD28371; human: DQ327728). The asterisks indicate identical amino acid residues in all the sequences.

The selected significance level was $P<0.05$.

Results

Cloning of CaSR from the scales of goldfish

PCR products (457 bp, underlined region in Fig.1) were obtained by PCR amplification. Using the obtained PCR product, RACE cloning was performed. As a result, the partial cDNA sequence of CaSR was determined (Fig. 1). The molecular structure of human CaSR and the cloned region of goldfish CaSR were shown in Fig. 2. Human CaSR consists of 1078-amino acids (aa) and has ligand-binding domain (20-530 aa), cysteine-rich region (538-591 aa) and transmembrane domain (622-860 aa). The cloned region of goldfish CaSR (579-837 aa) contained most of the transmembrane domain.

Structural comparison of goldfish CaSR with other CaSRs (zebrafish: XP_689097; salmon: NP_001119703; lizard: XP_003223807; pig: XP_003132690; mouse: AAD28371; human: DQ327728) was indicated in Figure 3. Most of amino acids were conserved among these vertebrates.

Effect of acceleration loading by vibration on CaSR mRNA expression in the scales of goldfish

The results of acceleration loading by vibration on CaSR mRNA expression are shown in Figure 4. The mRNA expression of CaSR was increased by hyper-loading in the regenerating scales of goldfish. Significant difference between control and experimental group was observed at 6 and 24 h of incubation.

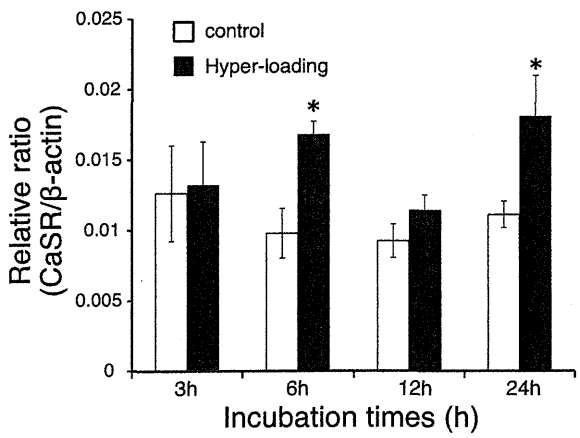

Fig. 4. Effect of acceleration loading by vibration on CaSR mRNA expression in the regenerating scales of goldfish. Each column and vertical line represent the mean ± S.E.M. (n = 6 samples; one sample from one goldfish). *$P<0.05$ versus control by paired *t*-test.

Discussion

We successfully determined the partial sequence of CaSR in the scales of goldfish. The putative goldfish CaSR of 258-amino acids has high sequence identity to zebrafish CaSR (XP_689097, 96%), salmon CaSR (NP_001119703, 92%), gilt-head bream CaSR (CAC41352, 91%), tilapia CaSR (XP_003446893, 90%), fugu CaSR (BAA26122, 89%), flounder CaSR (FJ755006, 89%), lizard CaSR (XP_003223807, 82%), cattle CaSR (DAA33414, 84%), pig CaSR (XP_003132690, 84%), mouse CaSR (AAD28371, 83%), and human CaSR (DQ327728, 84%). Among these vertebrates, we found that CaSR sequences are well-conserved at least in the region of 258-amino acids and suggesting that CaSR sequences possess evolutionary conserved property which may have important biological function in vertebrates.

A regulatory mechanism(s) governing CaSR mRNA expression is essential to understand the physiological significance of goldfish CaSR. Recently, Sun *et al.* (2012) reported that mechanical stretch induced calcium efflux from bone matrix and stimulated osteoblasts, and suggested that bone matrix acts as an intermediate mechanochemical transducer which converts the mechanical strain into a chemical signal in terms of the calcium efflux. There are several reports which show that the teleost scale contains osteoblasts, osteoclasts, and the bone matrix (Bereiter-Hahn and Zylberberg, 1993; Suzuki *et al.*, 2000; Yoshikubo *et al.*, 2005; Suzuki *et al.*, 2007; Ohira *et al.*, 2007). As the scale is equipped with the bone matrix, osteoblasts in the scales sensitively may respond to acceleration loading.

Calcium is an essential mineral to maintain cell viability and, ultimately, animal life. In all vertebrates, blood calcium levels are strictly kept at a constant concentration (around 2.5 mM) in spite of changing the internal milieu or external environment (Dacke, 1979). To regulate the blood calcium in teleosts, the scales have an important role because teleost scales are known to work as a potential internal calcium reservoir, similarly to those in endoskeletons of mammals, especially during increasing demand of calcium, such as sexual maturation or starvation (Yamada, 1961; Berg, 1968; Bereiter-Hahn and Zylberberg, 1993; Mugiya and Watabe, 1977). We recently detected cathepsin K and tartrate-resistant acid phosphatase mRNA expression in the scale osteoclasts (Azuma *et al.*, 2007). In osteoblasts as well, we detected osteoblast-specific markers, such as runt-related transcription factor 2, osterix, type 1 collagen, alkaline phosphatase, osteocalcin, and the receptor activator of the NF-κB ligand (Thamamongood *et al.*, 2012). Therefore, the features of osteoclasts and osteoblasts in scales are quite similar to those in mammals. Calcium signal is essential for the proliferation and differentiation in mammalian osteoblasts (Theman and Collins, 2009; Dvorak-Ewell *et al.*, 2011), suggesting that extracellular calcium ion production occurs from the bone matrix of goldfish scales for conducting calcium signaling to osteoblasts *via* CaSR. We are currently developing an original array system for goldfish on the basis of Expressed Sequence Tag analysis. In the future study, we will be able to examine the detail mechanism including calcium signaling on osteogenesis using our original array system.

In conclusion, goldfish scales express CaSR like other vertebrates, and the expression of CaSR is regulated by loading. The expression of CaSR by loading suggests that scale is a good model for the analysis of bone metabolism under various gravity conditions.

Acknowledgments

This study was supported in part by grants to N.S. (Grant-in-Aid for Space Utilization by the Japan Aerospace Exploration Agency; Grant-in-Aid for Scientific Research [C] Nos. 21500404 and 24620004 by JSPS), to M.K. (Grant-in-Aid for Scientific Research [C] No. 24500541 by JSPS), to A.H. (Grant-in-Aid for Scientific Research [C] Nos. 21570062 and 24570068 by JSPS), to K.K. (Grant-in-Aid for Scientific Research [C] Nos. 21500681 and 24500848 by JSPS), to T.S. (Grant-in-Aid for Young Scientists [B] Nos. 22770069 and 40378568 by JSPS), and to K.H. (the Environment Research and Technology Development Fund [B-0905] sponsored by the Ministry of the Environment, Japan; Health, Labour Sciences Research Grants of the Ministry of Health, Labour and Welfare, Japan; Grant-in-Aids for Scientific Research [B] No. 21390034 and for Exploratory Research No.24651044 by JSPS). We are greatly thanks Mr. Nobuyuki Suzuki and Mrs. Reiko Suzuki for their assistance of keeping goldfish.

References

Azuma, K., Kobayashi, M., Nakamura, M., Suzuki, N., Yashima, S., Iwamuro, S., Ikegame, M., Yamamoto, T. and Hattori, A. (2007) Two osteoclastic markers expressed in multinucleate osteoclasts of goldfish scales. *Biochem. Biophys. Res. Commun.*, **362**, 594-600.

Bereiter-Hahn, J. and Zylberberg, L. (1993) Regeneration of teleost fish scale. *Comp. Biochem. Physiol. Part A*, **105**, 625-641.

Berg, A. (1968) Studies on the metabolism of calcium and strontium in freshwater fish I: relative contribution of direct and intestinal absorption. *Mem. Ist. Ital. Idrobiol.*, **23**, 161-196.

Brown, E.M., Gamba, G., Riccardi, D., Lombardi, M., Butters, R., Kifor, O., Sun, A., Hediger, M.A., Lytton, J. and Hebert, S.C. (1993) Cloning and characterization of an extracellular Ca^{2+}-sensing receptor from bovine parathyroid. *Nature*, **366**, 575-580.

Brown, E.M. and MacLeod, R.J. (2001) Extracellular calcium sensing and extracellular calcium signaling. *Physiol. Rev.*, **81**, 239-297.

Chenna, R., Sugawara, H., Koike, T., Lopez, R., Gibson, T.J., Higgins, D.G. and Thompson, J.D. (2003) Multiple sequence alignment with the clustal series of programs. *Nucleic Acids Res.*, **31**, 3497-3500.

Dacke, C.G. (1979) Calcium Regulation in Sub-Mammalian Vertebrates. London, Academic Press.

Dvorak-Ewell, M.M., Chen, T.H., Liang, N., Garvey, C., Liu, B., Tu, C., Chang, W., Bikle, D.D. and Shoback, D.M. (2011) Osteoblast extracellular Ca^{2+}-sensing receptor regulates bone development, mineralization, and turnover. *J. Bone Miner. Res.*, **26**, 2935-2947.

Gebken, J., Lüders, B., Notbohm, H., Klein, H.H., Brinckmann, J., Müller, P.K. and Bätge, B. (1999) Hypergravity stimulates collagen synthesis in human osteoblast-like cells: evidence for the involvement of p44/42 MAP-kinases (ERK 1/2). *J. Biochem.*, **126**, 676-682.

Godwin, S.L. and Soltoff, S.P. (2002) Calcium-sensing receptor-mediated activation of phospholipase C-γ1 is downstream of phospholipase C-b and protein kinase C in MC3T3-E1 osteoblasts. *Bone*, **30**, 559-566.